

## Synthesis of Multiwall Carbon Nanotubes by Inductive Heating CCVD

A.R. Biriş<sup>a,\*</sup>, A.S. Biriş<sup>b</sup>, D. Lupu<sup>a</sup>, S. Trigwell<sup>c</sup>, Z. U. Rahman<sup>d</sup>, N. Aldea<sup>a</sup>, P. Mărginean<sup>a</sup>

<sup>a</sup> *National Institute for Research and Development of Isotopic and Molecular Technologies,*

*P.O. Box 700, R-400293 Cluj-Napoca, Romania*

<sup>b</sup> *University of Arkansas at Little Rock, College of Science and Mathematics, Chemistry*

*Department, 2801 S. University Ave, Little Rock, AR, 72204, U.S.A,*

<sup>c</sup> *Electrostatics & Surface Physics Laboratory, Mail code: YA-C2-T, Kennedy Space Center,*

*FL 32899*

<sup>d</sup> *Advanced Materials Processing and Analysis Center, University of Central Florida, 12443*

*Research Pkwy., Suite 304, Orlando, FL, 32826*

### Abstract

The CCVD syntheses of MWCNTs from acetylene on Fe:Co:CaCO<sub>3</sub> and Fe:Co:CaO were performed using two different methods of heating: outer furnace and inductive heating. The comparative analysis of the MWCNTs obtained by the two methods show that the tubes grown in inductive heating have smaller diameters (5-25 nm), with fewer walls and aspect ratio of the order of hundreds. The ratio of outer to inner diameter (od/id) is ranging between 2 and 2.5. Inductively assisted CCVD is a very attractive method because of the major advantages that it presents, like low energetic consumption, thinner, well crystallized and more uniform tubes.

Keywords: A. Carbon nanotubes; B. Chemical vapor deposition, Induction heating

---

\* Corresponding author. Fax: + 261.584037

E-mail address: biris@oc1.itim-cj.ro (A.R. Biriş)

## Introduction

In the last 14 years since the discovery of the carbon nanotubes [1], they became a key component of nanotechnology [2], being currently among the most intensively studied materials.

Among the synthesis methods of carbon nanotubes, the catalytic chemical vapor deposition (CCVD) is the most commonly used, due its versatility in the growth morphology control of the carbon nanostructures by monitoring the reaction conditions (catalysts, temperature, composition and flow rate of the carrier gas, and hydrocarbons, etc). It is considered as the most promising method for large-scale production of carbon nanostructures.

Following the growth process by CCVD method, the carbon nanotubes have to be purified in order to remove the catalyst particles and the carbon byproducts without destroying the morphology of the nanotubes. In the last years the attention has been focused on finding performant catalysts for high quality production of carbon nanotubes, able to allow the removal of both the metal nanoparticles and the oxide support in a single purification step, generally by dissolution in diluted acids. Much progress has been made using  $\text{Co}_3\text{O}_4/\text{MgO}$  [3] and  $\text{Fe:Co}/\text{CaCO}_3$  [4] catalysts.

The increasing need for carbon nanotubes (both SWCNTs and MWCNTs) resulted in the development of techniques for scale-up the continuous synthesis by CCVD [4] and of new high-yield catalysts [5-7].

The synthesis of carbon nanotubes by inductively assisted CCVD has lower energetic consumption and the overall reaction time is significantly reduced with direct impact on the final production price of the nanotubes. In inductive heating the heat transfer flows from the susceptor to the catalyst which are in direct contact and requires a smaller number of intermediary steps compared with the resistive heating in outer furnace. The thermal fluctuations for the inductively enhanced CCVD are much smaller and the temperature can be

controlled more accurately. The inductive heating was used for carbon fibers production [8] and for susceptor heating in laser ablation SWNTs synthesis [9]. Lupu et al. reported for the first time the growth of carbon nanotubes (SWCNTs and MWCNTs) and carbon nanofibers by inductive heating while using a number of catalysts and different carbon sources [10,11]. Later, this method was used to produce SWCNTs by the catalytic decomposition of alcohol on a bimetallic catalyst of Fe/Co on zeolite support [12].

This paper reports experimental results for MWCNTs synthesis by inductive heating assisted CCVD. A catalyst reported by Couteau et al [4] was selected for our experiments, using the same conditions, for a comparative study of the outer furnace and induction heating effects and also of the catalyst support ( $\text{CaCO}_3$  and  $\text{CaO}$ ) effects.

## Experimental

The Fe:Co/ $\text{CaCO}_3$  catalyst was prepared as described in the literature [4] by impregnation.  $\text{Fe}(\text{NO}_3)_3 \cdot 9\text{H}_2\text{O}$  and  $\text{Co}(\text{CH}_3\text{COO})_2 \cdot 4\text{H}_2\text{O}$  salts were dissolved in distilled water followed by the introduction of  $\text{CaCO}_3$  under continuous stirring. During the preparation of the catalyst, the pH was kept constant at 7.2 by adding  $\text{NH}_4\text{OH}$ . The ratios of  $\text{Fe}(\text{NO}_3)_3 \cdot 9\text{H}_2\text{O}$ ,  $\text{Co}(\text{CH}_3\text{COO})_2 \cdot 4\text{H}_2\text{O}$ , and  $\text{CaCO}_3$  were those corresponding to final composition Fe:Co/ $\text{CaCO}_3$  = 2.5:2.5:95 wt % (further referred to as  $\text{CaCO}_3$ ). The solvent was evaporated on a water bath the result product was dried over night at 130 °C followed by grinding into a mortar.

The Fe:Co/ $\text{CaO}$  catalyst was obtained by thermal decomposition of Fe:Co/ $\text{CaCO}_3$  catalyst at 830 °C with the final result Fe:Co/ $\text{CaO}$  = 4.3:4.3:91.4 wt.% (further referred to as  $\text{CaO}$ ).

The MWCNTs were synthesized on  $\text{CaCO}_3$  and  $\text{CaO}$  catalysts by CCVD method in a fixed-bed flow reactor by decomposing acetylene at 720 °C in both outer furnace (OF) and inductively heated (IH) regime.

100 mg of catalyst were placed in a graphite boat, which was inserted in a quartz tube (28 mm inner diameter and 1 m length) and heated at the reaction temperature in nitrogen flow (200 ml/min). When the boat reached reaction temperature, acetylene was introduced (3.3 ml/min); the reaction time was 30 min for all the experiments after which acetylene flow was stopped and the sample cooled in nitrogen flow.

For inductive heating the outer furnace was replaced by a nine-coil inductor of 45 mm inner diameter and 80 mm length connected to a high frequency generator (1.3 MHz). The inductive heating ensured a very uniform heating of the susceptor (the same boat used in outer furnace technique) and the temperature was monitored with an optical pyrometer.

In some experiments the  $\text{CaCO}_3$  catalyst was activated prior to the CCVD synthesis (further referred to as  $\text{CaCO}_3 + \text{H}_2$ ). The activation was done "in situ" at 400 °C by a mixture of nitrogen (200 ml/min) and hydrogen (18 ml/min) for 30 min. After the activation time, the hydrogen flow was stopped and the temperature was raised to 720 °C and acetylene flow started for CCVD synthesis.

To produce the CaO catalyst, 150 mg of  $\text{CaCO}_3$  catalyst was placed in the susceptor, heated inductively at 830 °C in nitrogen for 30 minutes, followed by the adjustment of the temperature to 720 °C and the introduction of acetylene

The scheme of the experimental se-up used for producing the carbon nanotubes by CCVD method with inductive heating is shown in Fig. 1.

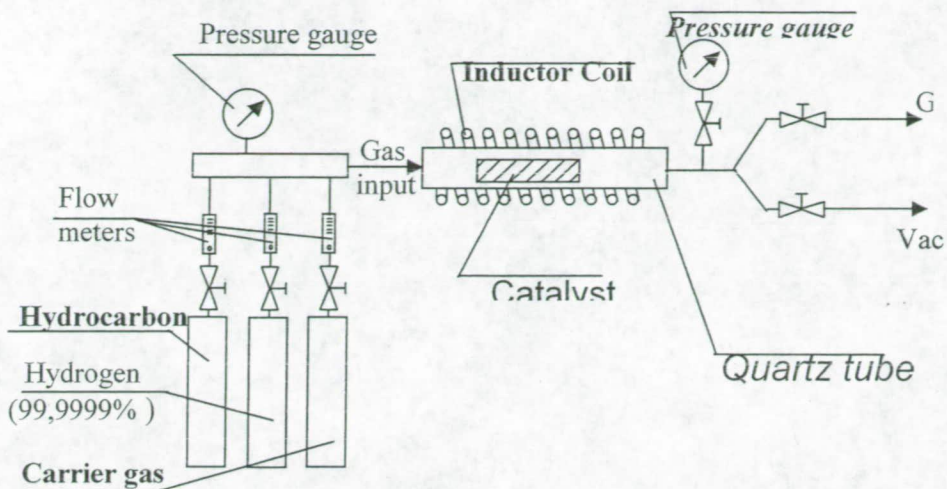


Fig.1. Scheme of the experimental se-up for inductive heating assisted CCVD syntheses of carbon nanotubes.

The products were purified by sonication in  $\text{HNO}_3$  (30 %) for 30 min, filtered, washed with distilled water and dried at  $130\text{ }^\circ\text{C}$ . The efficiency of the reaction is defined as per cent ratio between the mass of product obtained after purification and the initial mass of catalyst.

For the catalysts characterization several techniques were used thermogravimetric analysis (TGA) (Mettler Toledo 815e), SEM and X – Ray diffraction (DRON 2).

The morphology of the carbon nanotubes was analyzed by High Resolution Transmission Electron Microscopy (FEI Tecnai F30 STEM).

## Results and Discussions

The thermal decomposition curve of the  $\text{CaCO}_3$  catalyst, Fig. 2, show several stages: the weight loss in the range  $100\text{-}150\text{ }^\circ\text{C}$  corresponding adsorbed water, the decomposition of the acetates at  $250\text{-}350\text{ }^\circ\text{C}$  and the drastic weight loss between  $680\text{-}800\text{ }^\circ\text{C}$  due to the decomposition of calcium carbonate into calcium oxide and carbon dioxide [4]. The total

weight loss is 45.7% of the initial mass. The three stages of mass decrease are more visible in the first order derivative curve.

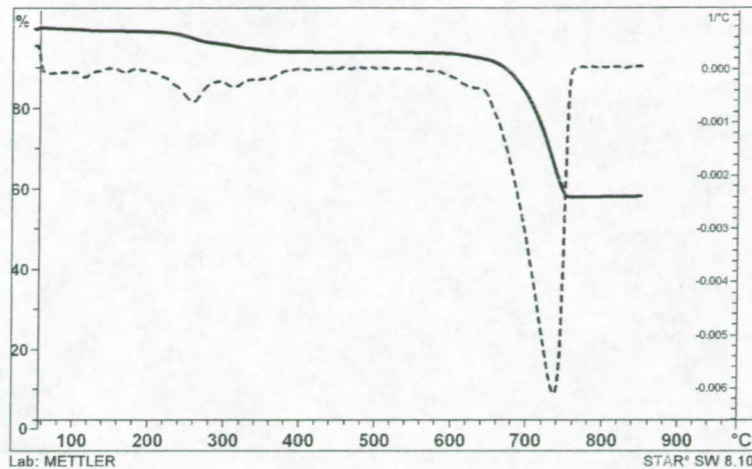
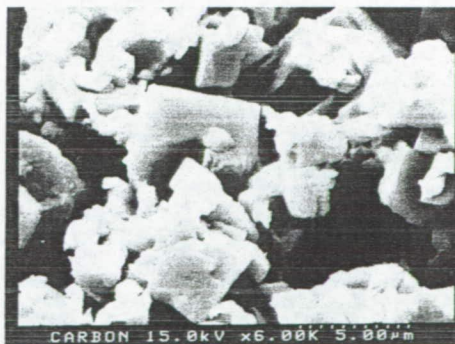
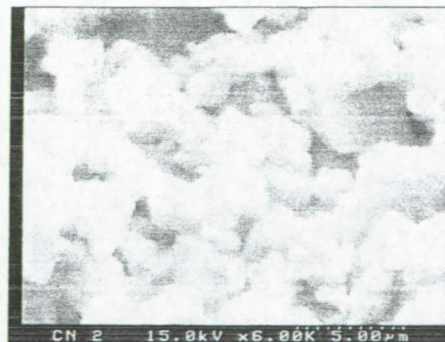


Fig.2. The thermal decomposition curve of the  $\text{CaCO}_3$  catalyst along with its first derivative curve.

Fig.3 presents the SEM images of the  $\text{CaCO}_3$  catalyst and the  $\text{CaO}$  catalyst. It can be observed that they have sponge-type morphologies but for the  $\text{CaO}$  catalyst the holes are smaller and more frequent. The  $\text{CaCO}_3$  catalyst (Fig. 3a) shows particles between 600-5000 nm with flat and smooth surfaces. The  $\text{CaO}$  catalyst (Fig. 3b) exhibits particles in the same range of dimensions with rough surfaces.



a)



b)

Fig.3. SEM images of the  $\text{CaCO}_3$  (a) and  $\text{CaO}$  (b) catalysts

The BET surface areas measured by krypton adsorption for the two catalysts are 6.2 m<sup>2</sup>/g for CaCO<sub>3</sub> and 6.3 m<sup>2</sup>/g for CaO respectively.

Figure 4 shows the powder X-ray spectrum for the CaO catalyst. The spectral lines correspond only to a CaO support and the catalytic metals are present in an oxidized state as Fe<sub>3</sub>O<sub>4</sub> and Co<sub>3</sub>O<sub>4</sub>, as identified by the corresponding spectral lines. The spectral peak corresponding to a diffraction angle of  $2\theta \approx 51^\circ$  is attributed to the spinel CaFe<sub>2</sub>O<sub>4</sub> formed most probably due to the thermal treatment.

The peaks corresponding to the Fe<sub>3</sub>O<sub>4</sub> and Co<sub>3</sub>O<sub>4</sub> compounds were approximated based on a generalized Fermi distribution that describes their degree of asymmetry and the calculation for the integral widths for the peaks were done by solving the Fourier deconvolution equation [13,14].

For both CaCO<sub>3</sub> and CaO catalysts, the average dimensions of the Fe<sub>3</sub>O<sub>4</sub> and Co<sub>3</sub>O<sub>4</sub> crystallites corresponding to each identified diffraction peak were obtained by using the Scherrer equation and range between 41–47 nm for Fe<sub>3</sub>O<sub>4</sub> and between 10–36 nm for Co<sub>3</sub>O<sub>4</sub>,

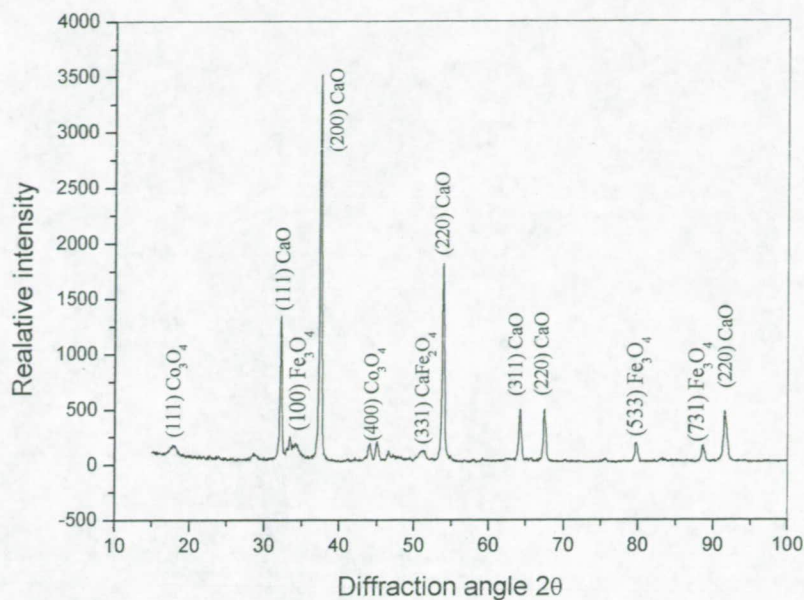


Fig. 4. The X-Ray powder diffraction spectrum for the CaO catalyst

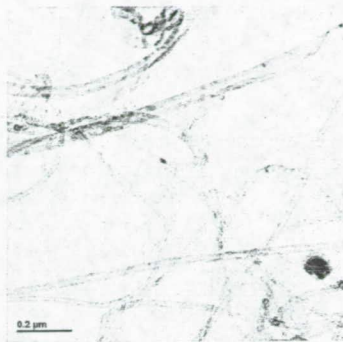
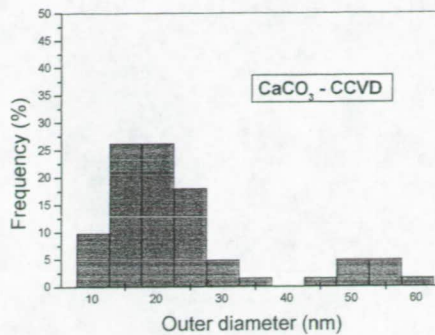
The low magnification TEM images as well as the diameter histograms (each histogram based on the analysis of over 100 individual nanotubes) of the multiwall carbon nanotubes grown on the  $\text{CaCO}_3$  and CaO in different conditions are shown in Fig.5.

The histogram for the nanotubes grown on  $\text{CaCO}_3$  catalyst in outer furnace (Fig. 5a) shows the presence of two groups of MWCNTs. The first one comprises the large majority of the nanotubes ( $\sim 86\%$ ) with outer diameter 8-35 nm and the second one much less abundant ( $\sim 14\%$ ) in the range of 40-60 nm outer diameter. These results can be explained by the partial decomposition of the  $\text{CaCO}_3$  catalyst when the temperature increases from 680 to 720 °C (see Fig.1): in this situation, the nanotubes are grown on a mixture of  $\text{CaCO}_3$  and CaO supported catalysts, as revealed by diameter distribution histogram.

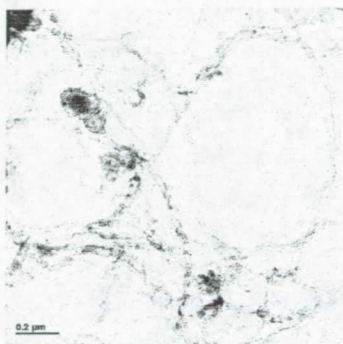
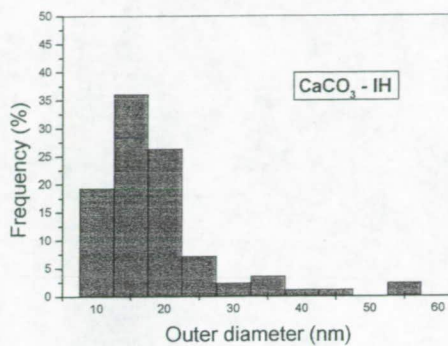




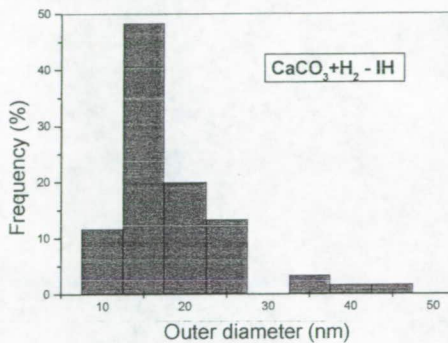
**a**



**b**



**c**



**d**

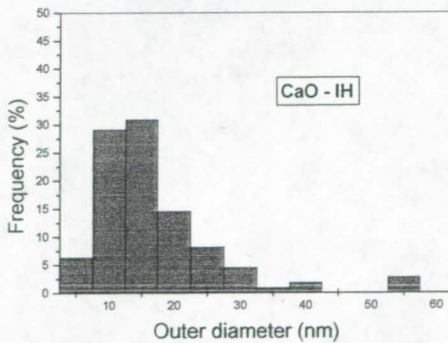


Fig.5. Low resolution TEM images and the diameter histograms for the multi wall carbon nanotubes synthesized from acetylene at 720 °C in different conditions: CaCO<sub>3</sub> (OF) (a), CaCO<sub>3</sub> (IH) (b), CaCO<sub>3</sub>+H<sub>2</sub> (IH) (c), and CaO (IH) (d).

Generally, for the nanotubes grown by inductive heating (Fig. 5 b-d), a decrease of the outer diameter is observed (over 90 % of the nanotubes having outer diameters 5-25 nm). Two hypotheses may be imagined:

i) The surface diffusion rate of Fe(Co) species on the support increases with temperature resulting in an increase of the nanoparticle catalyst (NP) with increasing annealing time [15]. The carbon nanotubes outer diameter follows the NPs dimension [16-18]. With the inductive heating a much faster heating rate is possible, the reaction temperature is reached in few dozens of seconds. The fast IH, with very short annealing time, does not allow significant increase of NPs average size so that nanotubes of lower outer diameter are obtained.

ii) The exothermal reaction of carbon graphitization supplies a large amount of thermal energy to the catalyst nanoparticle and since the heat transfer to the low thermal conductivity oxidic support is limited, it could be possible that the metallic nanoparticles are supposed to a melting and reconstruction process [19]. The metallic character of the catalyst nanoparticles can determine an increase of their local temperature, induced by the RF skin currents. Therefore, a temperature difference might be present between the metallic species and the oxidic support of the catalysts that have a lower thermal conductivity and represent a "bottleneck" for the transfer of heat [19]. A higher local temperature can result in a higher growth rate of the nanotubes with smaller diameters as reported in the literature [16, 20, 21].

Though the CaO catalyst was exposed to a 30 minute thermal treatment at 850 °C, with the possibility of larger metallic particles formation, the diameter distribution of the nanotubes was found to be relatively narrow (5-25 nm) as seen in Fig. 5d. This observation points the second hypothesis as more reliable for the growth of thinner nanotubes in inductively heated CCVD. This effect can be exploited also for other catalyst systems where higher temperatures can be reflected in morphological and structural changes of the catalyst support.

The analysis of the TEM images shows that most of the nanotubes have lengths larger than 2-3  $\mu\text{m}$ , which allows the conclusion that the aspect ratio for these nanotubes is of the order of hundreds. Another characteristic that needs to be observed is the diameter uniformity over the entire length of the nanotubes. Generally there were not observed too many catalyst particles encapsulated; the number of the metallic nanoparticles encapsulated is slightly larger for the  $\text{CaCO}_3$  catalyst.

Figures 6 present the high resolution TEM pictures for the carbon nanotubes synthesized by inductively heated CCVD on the  $\text{CaCO}_3$  catalyst without (a) and with (b) hydrogen activation. All the HRTEM images have shown that the inductively grown carbon nanotubes are rather well crystallized with a relatively low number of carbon walls (7 – 12 walls) and with outer to inner diameter ratios (od/id) ranging between 2 and 2.5. The nanotubes grown with IH are generally thinner and have a fewer walls compared with those grown with outer furnace.

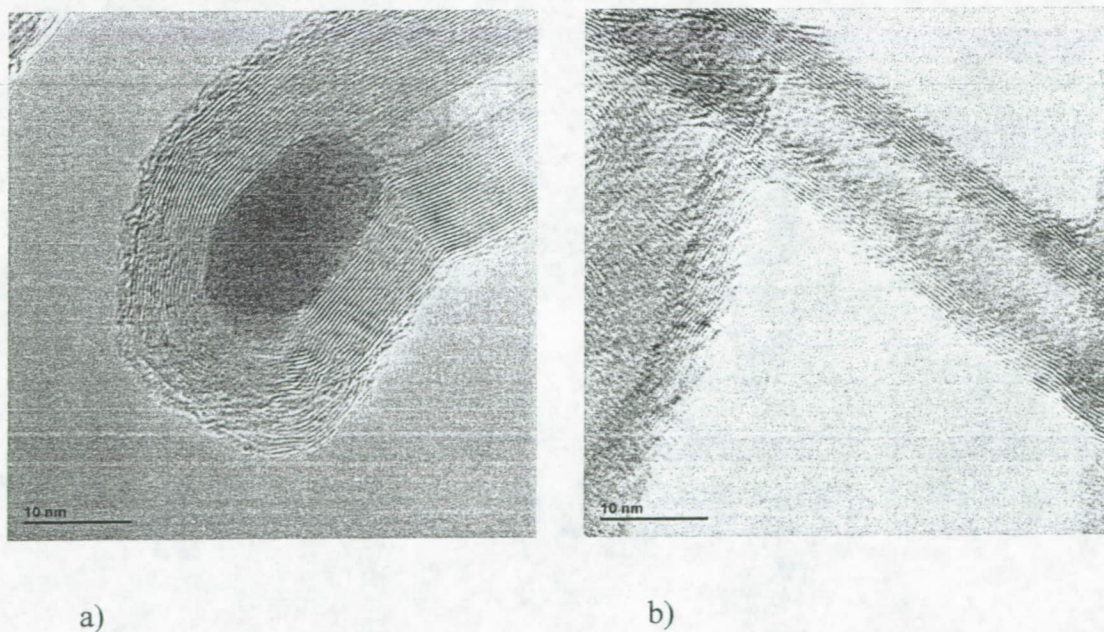


Fig. 6. HRTEM images of the carbon nanotubes grown on the  $\text{CaCO}_3$  catalyst without (a) and with (b) prior hydrogen activation

It should be mentioned that no morphological or structural differences were observed between the nanotubes that were grown on catalysts with or without prior hydrogen activation, another reason why this catalyst is suitable for continuous processes since it doesn't require activation.

Synthesis efficiency values relative to the  $\text{CaCO}_3$  catalyst are presented in Table 1.

Table 1. Synthesis efficiency values for multi wall carbon nanotubes grown in different conditions on the  $\text{CaCO}_3$  and  $\text{CaO}$  catalysts.

Sinteza	$\text{CaCO}_3$ (OF)	$\text{CaCO}_3$ (IH)	$\text{CaCO}_3+\text{H}_2$ (IH)	$\text{CaO}$ (IH)
$\eta$ (%)	87	78	74	26
[% gC/mol Ca]	91.6	82.2	78	27.4

As the surface areas of  $\text{CaCO}_3$  and  $\text{CaO}$  are practically the same, the much lower yield for  $\text{CaO}$  catalyst are consistent with the recent observations of Magrez et al [22] that the evolved  $\text{CO}_2$  from  $\text{CaCO}_3$  during the reaction is directly involved in the growth process for CCVD synthesis.

### Conclusions

The MWCNTs were prepared from acetylene at  $720^\circ\text{C}$  on the  $\text{Fe:Co/CaCO}_3$  and  $\text{Fe:Co/CaO}$  catalyst by using CCVD with heating with outer furnace and inductive heating using the same reaction conditions as reported by Couteau et al. [4].

The comparison between the MWCNTs characteristics synthesized by outer furnace and inductive heating shows that the inductive heating produces carbon nanotubes of smaller average diameter with fewer walls, and aspect ratio in the range of hundreds.

The comparative analysis of the yield for syntheses on  $\text{CaCO}_3$  and  $\text{CaO}$  is in good agreement with recently reported results [22], the participation of  $\text{CO}_2$  (resulting from  $\text{CaCO}_3$  support decomposition) in the growth process via a reaction with acetylene.

The inductively assisted CCVD has some major advantages over the classical CCVD: significantly lower energetic consumption, lower overall reaction time, much faster heating rate, possibility of visual inspection of the reaction, easier implementation of continuous production regime [23].

### References

- [1]. Iijima S. Helical microtubules of graphitic carbon. *Nature* 1991;353:56-58.
- [2]. Ando Y, Zhao X, Sugai T, Kumar M. Growing carbon nanotubes. *Materialstoday* 2004, October:22-29.
- [3]. Soneda Y, Duclaux L, Béquin F. Synthesis of high quality multi-walled carbon nanotubes from the decomposition of acetylene on iron-group metal catalysts supported on MgO. *Carbon* 2002;40:965-969.
- [4]. Couteau E, Hernardi K, Seo JW, Thiên-Nga L, Mikó Cs, Gaál R, et al. CVD synthesis of high-purity multiwalled carbon nanotubes using  $\text{CaCO}_3$  catalyst support for large-scale production. *Chem. Phys. Lett.* 2003;378:9-17.
- [5]. Xu JM, Zhang XB, Li Y, Tao XY, Chen F, Li T, et al. Preparation of  $\text{Mg}_{1-x}\text{Fe}_x\text{MoO}_4$  catalyst and its application to grow MWNTs with high efficiency. *Diamond & Related Materials* 2004;13:1807-1811.
- [6]. Li Y, Zhang XB, Tao XY, Xu JM, Huang WZ, Luo JH, et al. Mass production of high-quality multi-walled carbon nanotubes bundles on a Ni/Mo/MgO catalyst. *Carbon* 2005;43:295-301.

- [7]. Hata K, Futaba DN, Mizuno K, Namai T, Yamura M, Iijima S. Water-Assisted Highly Efficient Synthesis of Impurity-Free Single-Walled Carbon Nanotubes. *Science* 2004;306:1362-1364
- [8]. Rebouilliant S, Peng JCM, Donnet J-B, Ryu S-K in *Carbon Fibers* edited by Donnet J-B, Wang TK, Rebouilliant S, Peng JCM, 3<sup>rd</sup> ed. 1998, Dekker M, Inc. New York, Cap. 7:488-490.
- [9]. Gennett T, Dillon AC, Alleman JL, Jones KM, Heben MJ. Laser synthesis of single-walled carbon nanotube utilizing high temperature induction heating. *Mat Res Soc Symp Proc* 2001;633:A2.3.1-6.
- [10]. Lupu D, Biriş AR, Mişan I, Mihăilescu G, Olenic L, Pruneanu S, et al. Synthesis of carbon nanostructures by induction heating assisted CCVD method. *Studia Univ. Babeş-Bolyai, Physica, Spec. Issue* 2003;1:142-146. Proc. of 3<sup>rd</sup> Conf. Isotopic and Molecular Processes, Cluj-Napoca, Romania, Sept. 25-27, 2003.
- [11]. Lupu D, Biriş AR, Jianu A, Bunescu C, Burkel E, Indrea E, et al. Carbon nanostructures produced by CCVD with induction heating. *Carbon* 2004;42:503-507.
- [12]. Okamoto A, Shinohara H. Control of diameter distribution of single-walled carbon nanotubes using the zeolite-CCVD method at atmospheric pressure. *Carbon* 2005;43:431-436.
- [13]. Aldea N, Tiuşan CV, Barz B. A New X-Ray Line Profile Approximation Used for the Evaluation of the Global Nanostructure of Nickel Clusters. *J. Opt. Adv. Mat.* 2004;6:225-235
- [14]. Aldea N, Gluhoi A, Mărginean P, Cosma C, Yaning X. Extended X-ray absorption fine structure and X-ray diffraction studies on supported nickel catalysts *Spectrochim. Acta B* 200;55:997-1008.

- [15]. Ruckenstein E, in Metal-support interactions in catalysis, sintering, and redispersion edited by Stevenson SA, Dumesic JA, Baker RTK, Ruckenstein E, 1987, Van Nostrand Reinhold Company Inc. Cap. 14:270.
- [16]. Zaikovskii VI, Chesnokov VV, Buyanov RA. The relationship between the state of active species in a Ni/Al<sub>2</sub>O<sub>3</sub> catalyst and the mechanism of growth of filamentous carbon. *Kinetics Catal* 2001;42(6):813-820.
- [17]. Liang Q, Gao LZ, Li Q, Tang SH, Liu BC, Yu ZL. Carbon nanotube growth on Ni-particles prepared in situ by reduction of La<sub>2</sub>NiO<sub>4</sub>. *Carbon* 2001;39:897-903.
- [18]. Sato S, Kawabata A, Nihei M, Awano Y. Growth of diameter-controlled carbon nanotubes using monodispersed nickel nanoparticles obtained with a differential mobility analyzer. *Chem. Phys. Lett.* 2003;382:361-366.
- [19]. Little RB, Mechanistic aspects of carbon nanotube nucleation and growth. *J. Cluster Sci.* 2003;14:135-185.
- [20]. Piao L, Li Y, Chen J, Chang L, Lin JYS. Methane decomposition to carbon nanotubes and hydrogen on alumina supported nickel aerogel catalyst. *Catalysis Today* 2002;74:145-155.
- [21]. Topasztó L, Kertész K, Vértesy Z, Horváth ZE, Koós AA, Osváth Z, et al. Diameter and morphology dependence on experimental conditions of carbon nanotube arrays grown by spray pyrolysis. *Carbon* 2005;43:970-977.
- [22]. Magrez A, Seo JW, Mikó C, Hernárdi K, Forró L. Growth of Carbon Nanotubes With Alkaline Earth Carbonate as Support. *J. Phys. Chem.* 2005;109:10087-10091.
- [23]. Biriş A.R., Lupu D.M., Biris A.S., Wilkes J.G., Buzatu D.A., Miller D.W., et al. "Apparatus and Methods of High Throughput Generation of Nanostructures by

induction heating and improvements increasing productivity while maintaining quality and purity, US Patent Application No: 15003 - 46705